Nanoscale

Accepted Manuscript

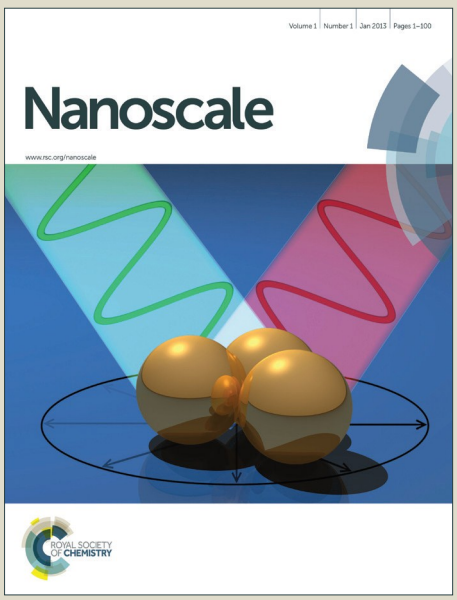

ROYAL SOCIETY OF CHEMISTRY

www.rsc.org/nanoscale

Journal Name

ARTICLE

pH-responsive biodegradable polymeric micelles with anchors to interface magnetic nanoparticles for MR Imaging in detection of cerebral ischemic area

Received 00th January 20xx,
Accepted 00th January 20xx

DOI: 10.1039/x0xx00000x

www.rsc.org/

HongYu Yang, [a] Moon-Sun Jang,[b] GuangHui Gao, [c] Jung Hee Lee *[b] and Doo Sung Lee*[a]

A novel type of pH-responsive biodegradable copolymer was developed based on methyloxy-poly(ethylene glycol)-block-poly[dopamine-2-(dibutylamino) ethylamine-$_L$-glutamate] (mPEG-b-P(DPA-DE)LG) and applied to act as an intelligent nanocarrier system for magnetic resonance imaging (MRI). The mPEG-b-P(DPA-DE)LG copolymer was synthesized by a typical ring opening polymerization of *N*-carboxyanhydrides (NCAs-ROP) using mPEG-NH_2 as a macroinitiator and two types of amine-terminated dopamine groups and pH-sensitive ligands were grafted onto a side chain by a sequential aminolysis reaction. This design greatly benefits from the addition of the dopamine groups to facilitate self-assembly, as these groups can act as high-affinity anchors for iron oxide nanoparticles, thereby increasing long-term stability at physiological pH. The mPEG moiety in the copolymers helped the nanoparticles to remain well-dispersed in an aqueous solution, and pH-responsive groups could control the release of hydrophobic Fe_3O_4 nanoparticles in an acidic environment. The particle size of the Fe_3O_4-loaded mPEG-b-P(DPA-DE)LG micelles was measured by dynamic light scattering (DLS) and cryo-TEM. The superparamagnetic properties of the Fe_3O_4-loaded mPEG-b-P(DPA-DE)LG micelles were confirmed by a superconducting quantum interference device (SQUID). T_2-weighted magnetic resonance imaging (MRI) of Fe_3O_4-loaded mPEG-b-P(DPA-DE)LG phantoms exhibited enhanced negative contrast with r_2 relaxivity of approximately 106.7 $mM^{-1}s^{-1}$. To assess the ability of the Fe_3O_4-loaded mPEG-P(DE-DPA)LG micelles to act as MRI probes, we utilized a cerebral ischemia disease rat model with acidic tissue. We found that a gradual change in contrast in the cerebral ischemic area could be visualized by MRI after 1 h, and maximal signal loss was detected after 24 h post-injection. These results demonstrated that the Fe_3O_4-loaded mPEG-b-P(DPA-DE)LG micelles can act as pH-triggered MRI probes for diagnostic imaging of acidic pathological tissues.

1. Introduction

Remarkable progress has been made in nanomedicine, and molecular imaging[1] has been widely explored because it is effective as a non-invasive assessment in biomedical applications, such as in the diagnosis of pathological tissues[2], recognition and discovery of disease[3] and real-time diagnostic visualization of the cellular functions of living organisms[4, 5]. In contrast to other imaging modalities such as X-ray scans[6, 7], CT [8, 9], PET[10, 11] and SPECT[12, 13], magnetic resonance imaging (MRI) is a powerful diagnostic technique that gives a clear visualization of damaged tissues and cells for clinicians and does not use ionizing radiation. Thus, MRI is highly suitable for routine diagnostic procedures[14-17]. However, higher MRI sensitivity is needed to accurately diagnose early stage cancers. One way to enhance MRI sensitivity is to use superparamagnetic iron oxide nanoparticles (SPIONs) as MRI contrast agents. The signal generated by the changing magnetization of the SPION tracers results in the occurrence of higher order harmonics in the excitation frequency, which facilitates quantitative mapping of the local distribution of the magnetic nanoparticles at high spatial and temporal resolution[18-20].

To the best of our knowledge, there are very few studies that have reported using polypeptide micelle systems to interface SPIONs in in vivo diagnoses. Polypeptides have been extensively studied as the most promising candidates for drug delivery due to their ability to undergo reversible secondary conformation transitions and/or hydrophilic-hydrophobic transitions in response to internal or external stimuli, and polypeptides are useful biocompatible and biodegradable polymers with structures that mimic natural proteins.[21-25] Because of their favorable characteristics, polypeptides are suitable for carrying Fe_3O_4 nanoparticles, which can be used in medicine and pharmaceutical science. However, the effective

[a] Theranostic Macromolecules Research Center, School of Chemical Engineering, Sungkyunkwan University, Suwon 440-746, Republic of Korea. E-mail: dslee@skku.edu
[b] Department of Radiology, Samsung Medical Center, Sungkyunkwan University School of Medicine and Center for Molecular and Cellular Imaging, Samsung Biomedical Research Institute, Seoul 135-710, Republic of Korea.
[c] Engineering Research Center of Synthetic Resin and Special Fiber, Ministry of Education, Changchun University of Technology, Changchun 130012, China
Electronic Supplementary Information (ESI) available: [details of any supplementary information available should be included here]. See DOI: 10.1039/x0xx00000x
*Co-Corresponding Author

integration of SPIONs into biological systems requires high loading efficacy, availability of SPIONs with homogeneous composition, stable dispensability in aqueous solutions and long-term stability[26-28]. To overcome these issue, Recently, Marcelo and coworkers[29] designed and prepared a well-defined hybrid polypeptide material to coat iron oxide nanoparticles, which were formed by *N*-carboxyanhydride ring-opening polymerization (NCA-ROP) using a dopamine biomimetic surface anchor as an initiator. Xu and coworkers[30] also reported a novel Fe_3O_4@SiO_2@poly-l-alanine peptide brush–magnetic microsphere (PBMMs), which was synthesized from amine-functionalized Fe_3O_4 through the surface-initiated polymerization of *N*-carboxyanhydrides, and these strategies have emerged as reliable approaches to improving the long-term structural stability of nanocarriers under physiological conditions. However, using surface-functionalized magnetic particles as initiators in the polymerization to form a covalently linked Fe_3O_4@polypeptide complex makes it difficult to control the chain length and molecular weight of the final polymers and leads to a broad molecular weight distribution. From a biomedical application perspective, controlling chain length and molecular weight of in the polymers is essential for many biological applications[31-33].

Moreover, it has been demonstrated that the pH is as low as 5.5-6.0 in the endosomes and 4.5-5.0 in the lysosomes of cancer cells, which contrasts with normal extracellular matrices and blood pH that are maintained at approximately 7.4.[34-36] For instance, some pathologic tissues (such as tumor and ischemic tissue) have more acidic pH than normal tissues [37,38]. The primary reason for an acidic pH is the accumulation of excess lactic acid, which is produced by the high rate of glycolysis in pathologic tissue [39]. Therefore, the low pH in the tumor or ischemic tissues is becoming a significantly stimuli-responsive environment for targeting. Thus, pH-sensitive nanomaterials have been exploited in the design of controlled imaging agents and/or hydrophobic drug that are released in the pathological area in respond rapidly to an acidic pH stimulus [40-42].

Based on the above mentioned reasons, a novel type of pH-responsive biodegradable polymeric micelle with an anchor was successfully fabricated based on methyloxy-poly(ethylene glycol)-block-poly[dopamine-2-(dibutylamino)ethylamine-*L*-glutamate] (mPEG-b-P(DPA-DE)LG). This novel pH-responsive polypeptide copolymer with an anchor was designed based on the following considerations: (i) This copolymer was synthesized via ring opening polymerization of *N*-carboxyanhydrides (NCAs-ROP) using mPEG-NH_2 as a macroinitiator and the chain length and molecular weight were controlled by changing the molar ratio of initiator to monomer [43], while the mPEG moiety in the copolymers helped the nanoparticles to disperse in aqueous solution and improved drug tolerance[44, 45]. (ii) Dopamine (DPA) is a widely used anchor molecule due to its ortho-dihydroxyphenyl (catechol) functional groups, which strongly coordinates to iron oxide nanoparticles surfaces[46]. Thus, dopamine was introduced into the copolymers and acted as a high-affinity anchor for iron oxide nanoparticles to increase the long-term stability at

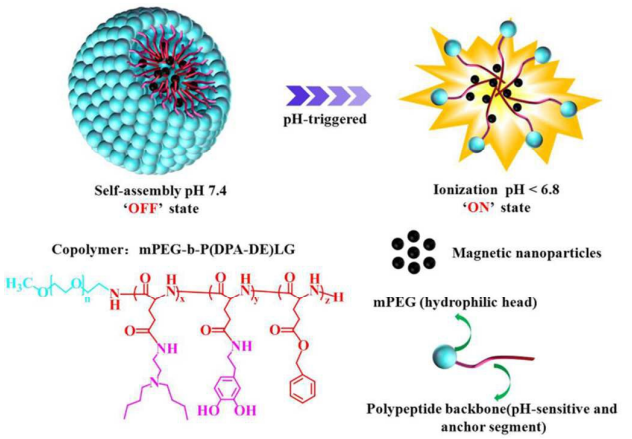

Scheme 1. Schematic illustration of the acidic pH-triggered Fe_3O_4-loaded mPEG-b-P(DPA-DE)LG micelles

physiological pH. (iii) As shown in Scheme 1, the hydrophobic Fe_3O_4 nanoparticles were encapsulated into the hydrophobic core of the polymeric micelles by using the anchor to interface with the surface of the Fe_3O_4 nanoparticles, and the resulting Fe_3O_4-loaded pH-responsive mPEG-b-P(DPA-DE)LG micelles could be used as MRI contrast agents that are targeted to acidic pH-triggered. The pH-sensitivity, hydrodynamic particle size, superparamagnetism and MRI relaxivity of the Fe_3O_4-loaded mPEG-b-P(DPA-DE)LG micelles were measured. Cell uptake and cytotoxicity were assayed. In addition, to test the Fe_3O_4-loaded mPEG-b-P(DPA-DE)LG micelles' abilities as acidic pH-triggered targeting agents for MRI, we employed a cerebral ischemia disease rat model with acidic tissue for in vivo evaluation.

2 Experimental section

2.1 Materials

L-Glutamic acid γ-benzyl ester, 2-hydroxypyridine, anhydrous tetrahydrofuran (THF), anhydrous chloroform, anhydrous N,N-dimethylformamide (DMF), α-pinene, doxorubicin hydrochloride (DOX), iron(III) acetylacetonate ($Fe(acac)_3$), chloroform-d, and phenyl ether were obtained from SigmaAldrich (USA). Methoxy polyethylene glycol amine (mPEG-NH_2, Mn=5000) was purchased from SunBio (Korea). Triphosgene, 2-(dibutylamino)ethylamine (DE), 1,2-hexadecanediol, oleic acid, and oleylamine were purchased from Tokyo Chemical Industry. Hexane, diethyl ether, and ethanol were obtained from Samchun (Korea). All the chemicals and solvents were used as received.

2.2 Synthesis of superparamagnetic iron oxide nanoparticles (SPIONs)

Superparamagnetic iron oxide nanoparticles were synthesized following a published procedure by Sun et al with slight modification.[47-49] Briefly, $Fe(acac)_3$ (2 mmol) was mixed in phenyl ether (20 mL) with 1,2-hexadecanediol (10 mmol), oleic acid (6 mmol), and oleylamine (6 mmol) under nitrogen flow and was rapidly heated to reflux at a heating rate of 20 °C /min

for a continuous reaction for 40 min at 265 °C. After cooling to room temperature, the mixture solution was treated with ethanol under air to yield a colloidal dark-brown precipitate. Centrifugation (10000 rpm, 10 min) was applied to remove any undispersed residue and solvent. The final product was redispersed into chloroform in the presence of oleic acid (~0.1 mL) and oleylamine (~0.1 mL) at a concentration of 25 mg/mL.

2.3 Synthesis of γ-Benzyl-$_L$-glutamate-N-carboxyanhydride (BLG-NCA)

γ-benzyl-$_L$-glutamate-*N*-carboxyanhydride (BLG-NCA) was synthesized according to our previous work with slight modification[50]. Briefly, 10 g of $_L$-glutamic acid γ-benzyl ester and 11.47 g of α-pinene were suspended in 90 mL of anhydrous THF under a nitrogen environment in a flame-dry three-neck flask. Triphosgene (6.255 g) was dissolved in 10 mL THF and slowly injected once into the reaction. The mixture was vigorously stirred at 55 °C until the milky solution turned clear within 0.5 h, after reaction for 2 hours. The product was precipitated by excessive n-hexane and then purified twice by recrystallization in 3:1 hexane/ethyl acetate (v/v). Yield: 96%. ^{1}H NMR (500 MHz, $CDCl_3$) ppm: 2.13 (s, -CHC**H**$_2$CH$_2$-), 2.61 (s, -CHCH$_2$C**H**$_2$-), 4.39 (s, -N**H**COO-), 5.21 (s, -C**H**$_2$C$_6$H$_5$), 7.35 (s, -C$_6$**H**$_5$).

2.4 Synthesis of methoxy poly(ethylene glycol)-block-poly(benzyl-$_L$-glutamate) (mPEG-b-PBLG)

mPEG-b-PBLG was synthesized by *N*-carboxyanhydrides ring-opening polymerization (NCAs-ROP) of BLG-NCA with mPEG-NH_2 as the macroinitiator. Typically, mPEG-NH_2 and BLG-NCA were dissolved in anhydrous chloroform using different molar ratios of the initiator to monomer. Then, the reaction mixture was stirred under nitrogen at 27 °C for 3 days. After the reaction was completed, the solution was concentrated by a rotary evaporator and precipitated in excess ethyl ether. The final polymer was dried in a vacuum oven for 3days. Yield: 87%. ^{1}H NMR (500 MHz, $CDCl_3$) ppm: 2.13(s, -CHC**H**$_2$CH$_2$-), 2.61(s, -CHCH$_2$C**H**$_2$-), 3.41(s, -OC**H**$_3$), 3.70(s, -OC**H**$_2$C**H**$_2$O-), 5.10(s, -C**H**$_2$C$_6$H$_5$), 7.35(s, -C$_6$**H**$_5$).

2.5 Synthesis of methoxy poly(ethyleneglycol)-block-poly[dopamine-2-(dibutylamino) ethylamine-$_L$-glutamate][mPEG-b-P(DPA-DE)LG]

mPEG-b-P(DPA-DE)LG copolymer was synthesized via a sequential aminolysis reaction of mPEG-b-PBLG with amine-terminated dopamine (DPA) and 2-(dibutylamino)ethylamine (DE). Briefly, mPEG-b-PBLG was dissolved in anhydrous N,N-dimethylformamide (DMF) (10 mL/1 g) under nitrogen environment in a round-bottom flask and immersed in an oil bath at 55 °C, followed by adding dopamine (DPA) (1× mol ratio to the ester groups of mPEG-b-PBLG) and 2-hydroxypyridine (5× mol ratio to the ester groups of mPEG-b-PBLG) for a reaction of 6 h. Then, 2-(dibutylamino)ethylamine (DE) (10× mol ratio to the ester groups of mPEG-b-PBLG) was added under the same conditions with continuous stirring for 12 h. After the reaction, the mixture was added dropwise to a cooled 0.5 M HCl solution (20 mL) and dialyzed against an aqueous solution of 0.01 M HCl solution for 2 days (MWCO=1,000 Da). The final products were obtained after lyophilization. Yield: 73%. ^{1}H NMR (500 MHz, $CDCl_3$) ppm: 0.78-(s, -C**H**$_3$ of DE), 1.21 and 1.3(s, -CH$_2$C**H**$_2$CH$_3$ and -C**H**$_2$CH$_2$CH$_3$ of DE), 2.41 and 2.89(s, -(CH$_2$)NC**H**$_2$CH$_2$- and -(CH$_2$)NCH$_2$C**H**$_2$- of DE), 2.99(s, -OC**H**$_3$), 3.50(s, -OC**H**$_2$C**H**$_2$O-), 5.1(s, -C**H**$_2$C$_6$H$_5$), 6.1-6.4 (s, -CH$_2$=C**H**CH-, -CH$_2$C**H**=CH- and =C**H**CO- of DPA).

2.6 Characterization of monomer and polymers

The molecular structures of the BLG-NCA, mPEG-b-PBLG and mPEG-b-P(DPA-DE)LG copolymers were characterized by ^{1}H-NMR using a 500 MHz spectrometer (Varian Unity Inova 500NB) in deuterated chloroform ($CDCl_3$) containing 0.03 v/v of tetramethylsilane as a reference at room temperature. The different components of the polymers were confirmed by checking the proton peak, and the molecular weights of the polymers were calculated by the integrated ratio of peak of the characteristic groups to the peak of the characteristic mPEG.

2.7 Preparation of Fe_3O_4-loaded mPEG-b-P(DPA-DE)LG micelles

Superparamagnetic iron oxide nanoparticles (SIONPs) were encapsulated into mPEG-b-P(DPA-DE)LG micelles by using a solvent-evaporation method[51]. Typically, 0.4 mL of colloidal SIONPs (25 mg Fe_3O_4/mL) in chloroform was added slowly to 5 mL of chloroform solution containing 100 mg of mPEG-b-P(DPA-DE)LG with vigorous stirring for 30 min under nitrogen at room temperature. Then, the mixture was incubated at 45 °C in a vacuum to evaporate chloroform thoroughly. An Fe_3O_4/ mPEG-b-P(DPA-DE)LG thin film was obtained and dispersed in 10 mL of PBS solution (pH 7.4) with gentle shaking for 40 min. A homogeneous dark-brown suspension was obtained by using syringe filters with a pore size of 200 nm (Millipore) to remove aggregated particles. Morphology was observed by cryogenic transmission electron microscopy (Cryo-TEM), and the images were recorded on a CCD camera (2k, Gatan) using a Tecnai F20 field emission gun electron microscope operated at 200 kV (FEI) in low-dose mode. The loading efficiency of Fe_3O_4 was calculated by the total added amount divided by the loading amount, and the Fe concentration was examined by inductively coupled plasma mass spectrometry (ICP-MS, Agilent 7500i).

2.8 Acid–base titration

The pH-buffering capacity of the mPEG-b-P(DPA-DE)LG copolymer was measured by an acid–base titration method. Typically, 30 mg of mPEG-b-P(DPA-DE)LG copolymer was dissolved in 30 mL of deionized water and titrated to around pH 3.0. To adjust the pH from 3.0 to 10.0, 0.01 mL of 0.1 M NaOH solution was added drop by drop, and the pH values were recorded to obtain the acid–base titration curve. The pKa value of the mPEG-b-P(DPA-DE)LG copolymer was estimated from the acid-base titration curve.

2.9 pH sensitivity and critical micelle concentration of mPEG-b-P(DPA-DE)LG copolymer

The pH sensitivity and CMC of the mPEG-b-P(DPA-DE)LG copolymer in an aqueous medium can be determined using pyrene as a fluorescence probe. The different pH values of the mPEG-b-P(DPA-DE)LG copolymer (1 mg/mL) in the pyrene-solubilized PBS solution were prepared by adjusting stepwise pH from 6.2 to 7.8 by using a 0.1 M NaOH solution. The concentration of the mPEG-b-P(DPA-DE)LG copolymer was varied from 2.0×10^{-3} to 1 mg/mL, and the concentration of pyrene was fixed at 1.0 μM. The fluorescence spectra were recorded using a fluorescence spectrometer (AMINCO, Bowman, Series 2) with an excitation wavelength of 392 nm. The emission fluorescence intensity at 337 and 334 nm was monitored. The CMC was estimated as the cross-point when extrapolating the intensity ratio I_{334}/I_{337} at low- and high-concentration regions.

2.10 The particle size and stability of Fe_3O_4-loaded mPEG-b-P(DPA-DE)LG micelles by DLS

The hydrodynamic radius of the mPEG-b-P(DPA-DE)LG micelles at different pH values and the particle size of the Fe_3O_4-loaded mPEG-b-P(DPA-DE)LG micelles were measured by dynamic light scattering (DLS) (Malvern Instrument, Series 4700) with a helium laser at 633 nm and a digital correlator. The correlation function was accepted when the difference between the measured and the calculated baselines was <0.1%. The scattering angle was fixed at 90°. Meanwhile, the stability of the Fe_3O_4-loaded mPEG-b-P(DPA-DE)LG micelles in PBS solution (pH 7.4) was characterized by DLS at different time intervals (1 day, 3 days, 5 days, 8 days, 10 days, 12 days and 15 days). Each sample was run in triplicate.

2.11 MR relaxivity test

To demonstrate the possibility of using the Fe_3O_4-loaded mPEG-b-P(DPA-DE)LG micelles as MRI contrast agents, the T_1 and T_2 relaxation times were measured at a series of different sample concentrations using a 3.0 T human clinical scanner (Philips, Achieva ver. 1.2, Philips Medical Systems, Best, The Netherlands) equipped with an 80 mT/m gradient amplitude and 200 ms/m slew rate. The T_1 relaxation time was measured by acquiring 17 gradient echo images at different inversion delay times using minimum inversion time of 87 ms with a phase interval of 264 ms, an in-plane image resolution=625×625 μm^2 and a slice thickness=500 μm. The images were fitted into a 3-parameter function to calculate T_1 values using the Matlab program. The T_2 measurement was performed by using 10 different echo times in a multislice turbo spin echo sequence (TR/TE=5000/20, 40, 60, 80, 100, 120, 140, 160, 180 and 200 ms, in-plane resolution=200×200 μm^2, slice thickness=500 μm). The images were fitted into a Levenberg-Marquardt function to calculate T_2 values using the Matlab program The specific relaxivities (r_1 and r_2) of Fe_3O_4-loaded mPEG-b-P(DPA-DE)LG micelles were generally determined by measuring the relaxation rate as a function of the iron concentration.

2.12 In vitro cytotoxicity assay

The cytotoxicity of the mPEG-b-P(DPA-DE)LG micelles and Fe_3O_4-loaded mPEG-b-P(DPA-DE)LG micelles against cultured HepG2 cells was evaluated in vitro using an MTT assay. All the samples with different concentrations were repeated at least four times to obtain the average value. Human hepatocellular carcinoma HepG2 cells were seeded onto coated metal surfaces into each well (96-well plates) at 37 °C in MEM (Gibco, Grand Island, NY) containing 10% (v/v) of FBS (Gibco, Grand Island, NY) and 1% (w/v) of penicillin-streptomycin and incubated overnight (5% CO_2). Subsequently, two types of samples were added into the wells to achieve different final concentrations (final concentrations were 32, 63, 125, 250 and 500 μg/mL). At 24 h post-treatment, the solution was transferred to a 96-well plate and the absorbance was measured at 450 nm using a Cell Counting Kit-8 (CCK-8, Dojindo, Kumamoto, Japan). Cell viability was calculated by comparing the MTT-treated cell solution with the control cell solution.

2.13 Release behaviour and Cellular uptake

In this investigation, a hydrophobic fluorescent agent doxorubicin (DOX) was selected to be encapsulated into the polymeric micelle for cellular uptake and release studies. DOX-loaded mPEG-b-P(DPA-DE)LG micelles were prepared as follows. Briefly, 1 mg DOX•HCl and 2 equivalents of TEA were mixed in 2 mL of tetrahydrofuran (THF) containing 10 mg mPEG-b-P(DPA-DE)LG. The mixture was stirred at room temperature under nitrogen for 30 min in the dark. After evaporating the solvents using a rotary evaporator, the polymer/DOX thin film was dispersed by adding 5 mL of deionized water with gentle shaking for 1 h. To obtain the DOX-loaded mPEG-b-P(DPA-DE)LG micelles, the mixture was dialyzed against a larger amount of deionized water for 24 h to remove free DOX. Next, the solution was filtered through a syringe filter (0.45 mm, Millipore) and freeze-dried. The drug loading content (DLC) and the drug loading efficiency (DLE) of DOX-loaded mPEG-b-P(DPA-DE)LG micelles were calculated based on the following equations:

DLE (wt%) = [weight of loaded drug/ weight of drug in feed]×100%

DLC (wt%) = [weight of loaded drug/ weight of drug-loaded micelle]×100%

The in vitro release profiles of DOX from the mPEG-b-P(DPA-DE)LG micelles were investigated in 50 mL centrifugal tubes containing 20 mL PBS at 37 °C under two different conditions, i.e., (i) PBS buffer solution (10 mM, pH 7.4) and (ii) PBS buffer solution (10 mM, pH 5.5). The DOX-loaded mPEG-b-P(DPA-DE)LG micelles suspension was added to cellulose ester membrane tubes (MWCO 3500 Da). The cellulose ester membrane tubes were immersed in 20 mL of a different PBS buffer solution and shaken at 37 °C. At certain time intervals, the cellulose ester membrane tubes were replenished with an equal volume of fresh medium. The amount of DOX was determined by UV-visible spectroscopy (excitation at 479 nm).

For cell uptake studies, human hepatocellular carcinoma HepG2 cells were seeded onto coverslips within 6-well plates (1 ×104 cells/well) in MEM (Gibco, Grand Island, NY)

containing 10% (v/v) of FBS (Gibco, Grand Island, NY) and 1% (w/v) of penicillin−streptomycin and incubated overnight (37 °C, 5% CO_2). Then, the cells were exposed to DOX-loaded mPEG-b-P(DPA-DE)LG micelles (both DOX concentration 10 μg L^{-1}) at 37 °C. After incubation for 1 and 24 h, the cells were fixed with 3.7% formaldehyde in PBS for 10 min, washed with PBS, and then soaked for 10 min in 3 mL of 4',6'-diamidino-2-phenylindole dihydrochloride (DAPI) and washed thrice with PBS before being mounted onto the slides. Cellular uptake was observed by a confocal laser scanning microscope (CLSM, LSM700 (CarlZeiss) X400) using a UV laser at wavelengths from 340 to 365 nm with excitation and emission wavelengths of 480 and 560 nm, respectively. The scale bar represents 20 μm.

2.14 In vivo MRI assessment

Adult rats (SD) of 280±20 g were treated according to the institutional guideline of Samsung Biomedical Research Institute for middle cerebral artery occlusion (MCAO) animal handling. The Fe_3O_4-loaded mPEG-b-P(DPA-DE)LG micelles (the final concentration of Fe_3O_4 was 3 mg/mL in a PBS solution) were injected into a tail vein line with a dose of 20 mg of Fe_3O_4 per kg of rat body weight for all experiments. For MRI, the animals were anesthetized and set into an MR-compatible cradle. During the MRI, the animals were anesthetized by 2% isoflurane in oxygen-enriched air via a facemask. Rectal temperature was maintained at 37±1 °C. To investigate the time course of the distribution of the Fe_3O_4-loaded mPEG-b-P(DPA-DE)LG micelles in the acidic pathologic area, MRI was performed before and at different times after administration of the samples to the MCAO animals. The in vivo MRI assessment was conducted using a 7.0 T MRI System (Bruker BioSpin, Fallanden, Switzerland) prepared with a 20 cm gradient set capable of providing 400 mT/m. A birdcage coil (72 mm i.d.) (Bruker-Biospin, Fallanden, Switzerland) was used for excitation, and a 4 channel phased array coil was used for receiving the signal for brain imaging. The Fe_3O_4-loaded mPEG-b-P(DPA-DE)LG micelles contrast enhanced the MRI that was obtained for each rat brain using a fast spin-echo T_2-weighted MRI sequence (repetition time (TR)/echo time (TE)= 4000/60 ms, number of experiment (NEX)= 1, echo train length= 1, 100 μm 3D isotropic resolution, field of view (FOV) = 3.56 × 2.56 × 2.56 cm^3, matrix size = 3.56 × 2.56 × 2.56 cm^3, slice selection direction= sagittal, and readout direction = head-to-foot) to evaluate the contrast. For the control experiment, a non-pH responsive Fe_3O_4-loaded mPEG-b-P(DPA)LG micelles was also used for in vivo imaging under the same conditions.

3 Results and Discussion

3.1 Synthesis and Characterization of BLG-NCA, mPEG-b-PBLG, and mPEG-b-P(DPA-DE)LG copolymers

The synthesis of BLG-NCA, mPEG-PBLG, and mPEG-b-P(DPA-DE)LG is shown in Scheme 2. First, the monomer of γ-benzyl-$_L$-glutamic acid N-carboxyl anhydride (BLG-NCA) was synthesized by phosgenation of L-Glutamic acid γ-benzyl ester using triphosgene. Briefly, $_L$-Glutamic acid γ-benzyl ester and α-pinene were added to 100 mL anhydrous THF at 50 °C in a 250 ml round-bottom flask, and a solution of triphosgene in 10 ml anhydrous THF was added dropwise. After 2.5 hours, the reaction was finished when the suspension became a completely clear solution, indicating the formation of BLG-NCA. The high purity of the BLG-NCA monomer was obtained by recrystallizing an ethyl acetate/hexane mixture three times, and its structure was confirmed by 1H-NMR, as shown in Supporting Information Figure S1. Secondly, mPEG-b-PBLG block copolymers in high yields were synthesized through ring-opening polymerization of N-carboxyanhydride (NCA-ROP) in anhydrous CH_3Cl_3 using mPEG-NH_2 as a macroinitiator. 1H NMR showed characteristic signals of mPEG (δ 3.41 and 3.70) and PBLG (δ 5.10 and 7.35) (See Supporting Information Figure S2), and the molecular weight and chain length of the block polymer could be controlled by varying the molar ratio of the monomer to initiator, with a higher ratio leading to a longer PBLG block (shown in Table 1). The degree of polymerization and molecular weight of mPEG-b-PBLG were calculated by comparing the signal integrated ratio of the mPEG methylene protons (δ 3.70) and benzyl methylene protons of PBLG (δ 5.10). Finally, the mPEG-b-P(DPA-DE)LG copolymers were obtained by a sequential aminolysis reaction of the flanking benzyl ester groups of mPEG-b-PBLG (mPEG-b-PBLG with a degree of polymerization of 60 [mPEG-b-$PBLG_{57}$] was employed in consideration of the hydrophobic/hydrophilic balance and hydrodynamic dimension of the peptide block of

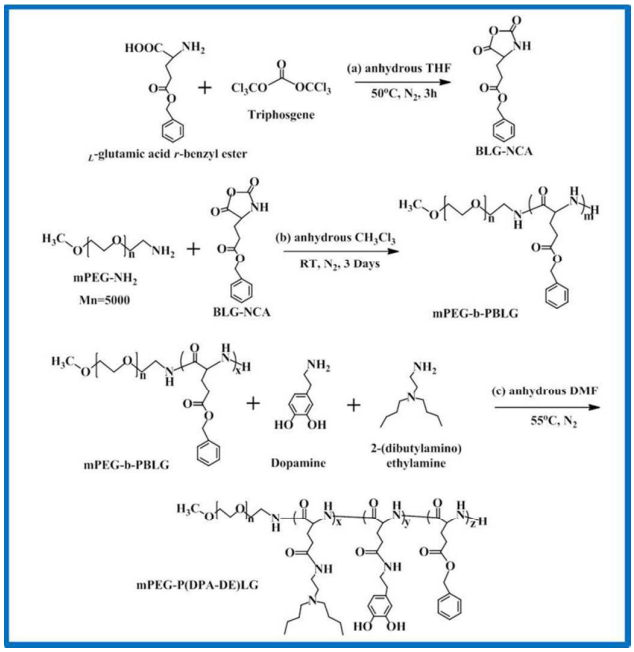

Scheme 2. Synthesis scheme of BLG-NCA (a), mPEG-b-PBLG (b) and mPEG-b-P(DPA-DE)LG (c)

Table 1 Feed ratios and characteristics of intermediated copolymers mPEG-b-PBLG

Entries	Reaction time	Molar ratio of initiator/monomer	Degree of polymerization	Mn[a]
mPEG-b-PBLG$_{51}$	72h	1/50	51	16169
mPEG-b-PBLG$_{57}$	72h	1/60	57	17483

[a]Calculated from ^{1}H NMR

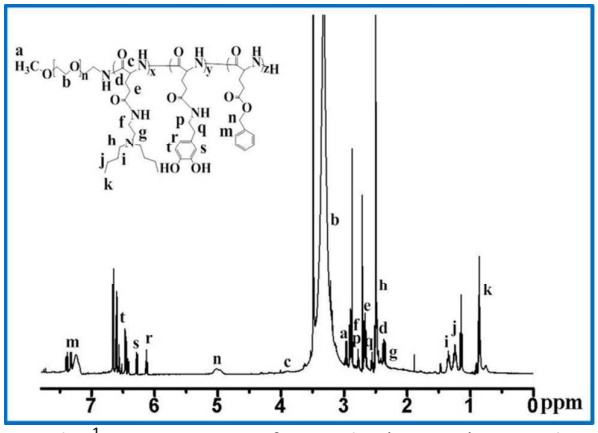

Fig. 1. the ^{1}H-NMR spectra of mPEG-b-P(DPA-DE)LG copolymer (500MHz, $CDCl_3$)

the ligand) with dopamine (DPA) and 2-(dibutylamino)ethylamine in the presence of 2-hydroxypyridine as a bifunctional catalyst to prevent chain scission of the polymer backbone (amide linkages of the polypeptide). Dopamine (DPA) and 2-(dibutylamino)ethylamine (DE) were then easily incorporated as a high-affinity anchor for iron oxide nanoparticles and an ionizable group to impart pH sensitivity to mPEG-b-P(DPA-DE)LG was confirmed by ^{1}H-NMR, as shown in Figure 1. The near disappearance of peaks at 5.1 and 7.3 ppm were attributed to the benzyl groups of mPEG-b-PBLG, and the new appearance of peaks were attributed to DPA (δ 6.1-6.4) and DE (δ 0.78, 1.21, 1.3 and 2.41) in the newly formed copolymers.

3.2 The characterization of the mPEG-b-P(DPA-DE)LG copolymer

The pH buffering properties of mPEG-b-P(DPA-DE)LG copolymer were checked by using an acid-base titration method, as shown in Figure 2. We can see that the mPEG-b-P(DPA-DE)LG copolymer dissolved in deionized water at pH 3.0, and the pH value increased rapidly from pH 3.0 to 6.5 by adding a 0.1 M NaOH solution. Afterwards, a buffering region appeared between pH 6.5 and 7.5, where the deprotonation of the tertiary amine began in mPEG-b-P(DPA-DE)LG. The pKa value of mPEG-b-P(DPA-DE)LG was calculated from the inflection point in the titration curve, which is listed in Table 2.

3.3 The pH-dependent micellization-demicellization behavior and CMC of the mPEG-b-P(DPA-DE)LG copolymer

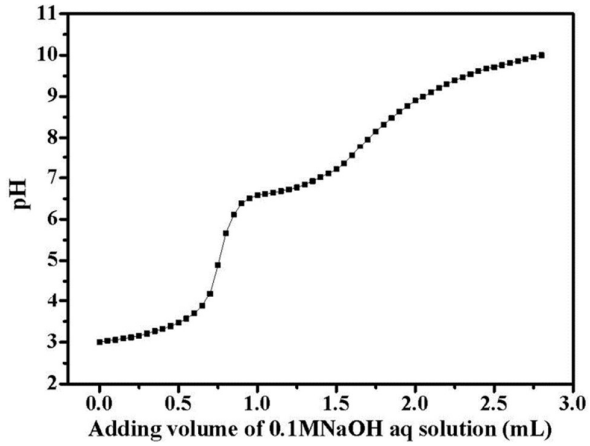

Fig. 2 Titration curves of mPEG-b-P(DPA-DE)LG copolymer (1 mg/mL in deionized water).

Table 2 Characteristics and properties of mPEG-b-P(DPA-DE)LG polymers and micelles

Entries	Conversion-DPA	Conversion-DE	pKa	CMC (mg/mL)	Loading Efficiency[a]	Size[b] (nm)	Mn[c]
mPEG-b-P(DPA-DE)LG	19%	70%	6.81	0.026	91.6%	46	20105

[a]Obtained from ICP-MS
[b]Obtained by DLS
[c]Calculated from ^{1}H NMR

The pH-dependent micellization-demicellization behavior of the mPEG-b-P(DPA-DE)LG copolymer was investigated by mPEG-b-P(DPA-DE)LG copolymer was investigated by fluorescence microscopy using pyrene as a polarity sensor. Pyrene is a relatively hydrophobic dye that preferentially localizes to a nonpolar environment and the absorption peak of pyrene in an aqueous medium is 337 nm, but shifts to 334 nm when pyrene is transferred into the hydrophobic domain of the micellar system. The typical fluorescence spectrum for mPEG-b-P(DPA-DE)LG at different pH values is listed in the corresponding Supporting Information Figure S3. Thus, the micellization/demicellization behavior of the mPEG-b-P(DPA-DE)LG copolymer was confirmed by monitoring the fluorescence plots of the ratio I_{337}/I_{334} at different pH values, as shown in Figure 3. When the pH was lower than 6.8, the ratio I_{337}/I_{334} of the mPEG-b-P(DPA-DE)LG copolymer was less than 1.0, indicating the destabilization of micellar structures due to the tertiary amine in mPEG-b-P(DPA-DE)LG being fully ionized and dissolved in aqueous media. However, as the pH increased from 6.8 to 7.2, a sharp transition occurred from a soluble state to a self-assembling micellar state, indicating a sharp micellization/demicellization transition, which implies that these polymeric micelles were quite sensitive to subtle changes in pH. When the pH was higher than 7.2, the ratio I_{337}/I_{334} values was greater than 1.0, indicating the formation of a large number of micelles from the mPEG-b-P(DPA-DE)LG copolymer in the aqueous medium.

The pH-dependent behavior of the mPEG-b-P(DPA-DE)LG copolymer in the aqueous medium was further investigated by DLS from pH 6.2-7.8. As shown in supporting information Figure S4, we found that the pH-sensitive mPEG-b-P(DPA-DE)LG copolymer

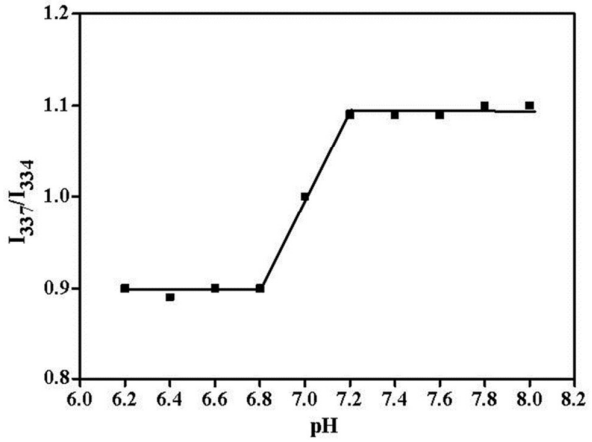

Fig. 3 The ratio I_{337}/I_{334} values of pyrene in mPEG-b-P(DPA-DE)LG polymer solution (1mg/mL) at different pHs

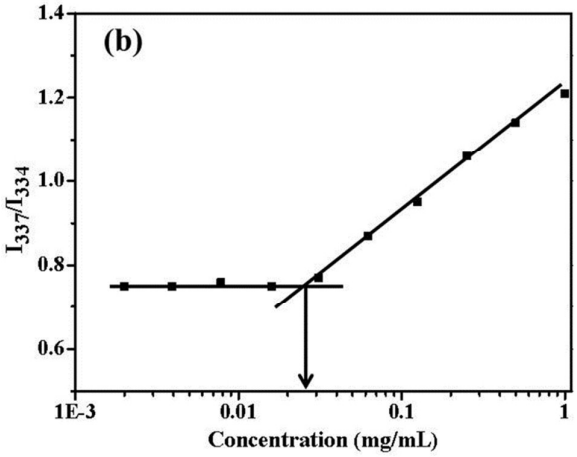

Fig. 4 Plots of the intensity ratio I_{337}/I_{334} of pyrene in mPEG-b-P(DPA-DE)LG copolymer solution of different concentrations.

could be dissolved completely at pH values lower than 6.8 in an aqueous medium due to the ionization of its tertiary amine groups, which led to the simultaneous demicellization of the micelles. As the solution pH increased from 6.8 to 7.0, the micelles showed an abrupt bump because of the loose micellar arrangement. As the pH increased from 7.0 to 7.8, the micelles exhibited a decrease in size due to the partial deionization of tertiary amine groups, which makes the micelle core more hydrophobic, causing it to shrink. Consequently, the mPEG-b-P(DPA-DE)LG copolymer exhibited a stable micellar state at physiological pH (7.4), and the size was approximately 46 nm.

Critical micelle concentration (CMC) is an important parameter to assess the stability of self-assembling polymeric micelles. The CMC value was investigated by using pyrene as a fluorescence probe in PBS (pH 7.4). The CMC value was determined by the intersection of the tangent point to the curve at the inflection with the horizontal tangent through the points at low polymer concentrations (Figure 4). According to the results, the CMC value was approximately 0.026 mg/mL for the mPEG-b-P(DPA-DE)LG copolymer. The fluorescence intensities of pyrene in the mPEG-b-P(DPA-DE)LG

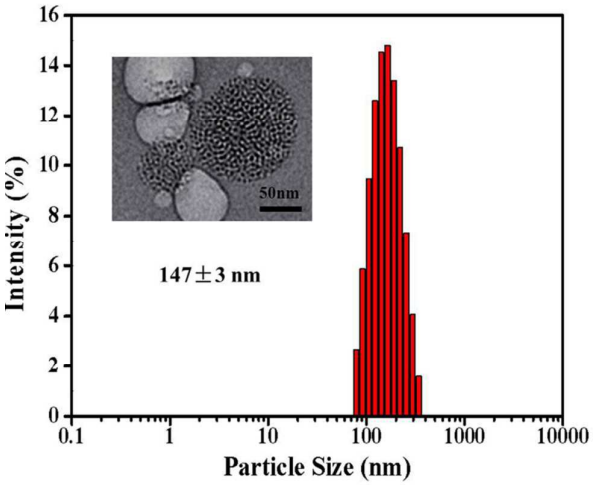

Fig. 5 The hydrodynamic particle size of Fe_3O_4-loaded mPEG-b-P(DPA-DE)LG micelles in PBS at pH 7.4 measured by DLS and cryo-TEM image.

solutions of different polymer concentrations are shown in Supporting Information Figure S4.

3.4 The characterization of Fe_3O_4-loaded mPEG-b-P(DPA-DE)LG micelles

The Fe_3O_4-loaded mPEG-b-P(DPA-DE)LG micelles were fabricated by self-assembly of Fe_3O_4 and the copolymer using a solvent evaporation method. The flanking dopamine groups acted as high-affinity anchors for the iron oxide nanoparticles to facilitate self-assembly. This led to the formation of micelles with Fe_3O_4 tightly packed within the hydrophobic core and a hydrophilic shell composed of hydrophilic blocks of the copolymer. Cryogenic transmission electron microscopy (Cryo-TEM) (Inserted Figure 5) images displayed tightly packed black Fe_3O_4 nanoparticles and indicated that the particle size of the Fe_3O_4-loaded mPEG-b-P(DPA-DE)LG micelles was ~ 120 nm. As shown in Figure 5, as expected, the hydrodynamic diameter as measured by DLS was 147 ± 3 nm, which is bigger than the average diameter measured in micrographs. This size is due to the increased intensity of scattering by large particles by DLS. Moreover, the Fe_3O_4 loading efficiency of the mPEG-b-P(DPA-DE)LG micelles was measured by ICP-MS, and the results are listed in Table 2.

The stability of the Fe_3O_4-loaded mPEG-b-P(DPA-DE)LG micelles was investigated by using DLS for two weeks in PBS (pH 7.4). As shown in Figure 6, the results indicated that the Fe_3O_4-loaded mPEG-b-P(DPA-DE)LG micelles show long-term stability with no significant change in the hydrodynamic diameter during the investigation period.

To investigate the superparamagnetic properties of the Fe_3O_4-loaded mPEG-b-P(DPA-DE)LG micelles, the lyophilized powder was analyzed using a superconducting quantum interference device (SQUID) at 300 K. The saturation loops of the Fe_3O_4-loaded mPEG-b-P(DPA-DE)LG micelles were determined by vibrating a sample magnetometer in the field H range of ± 70000 Oe at room temperature. As shown in Figure 7, the magnetization curve exhibited superparamagnetic properties due to the absence of a hysteresis loop, and the saturation magnetization value (Ms) was

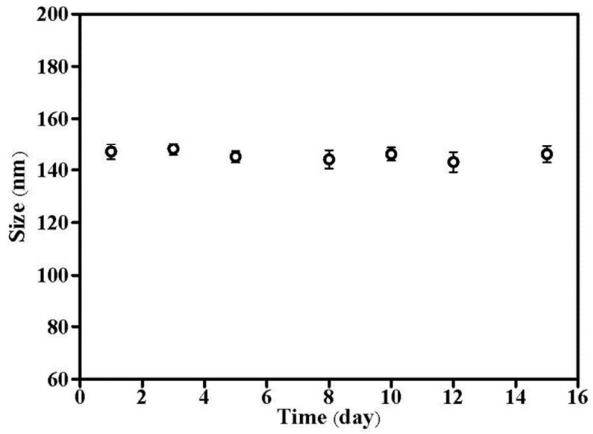

Fig. 6 The particles size of Fe_3O_4-loaded mPEG-b-P(DPA-DE)LG micelles are stable over 2 weeks in PBS at pH 7.4 as measurd by DLS.

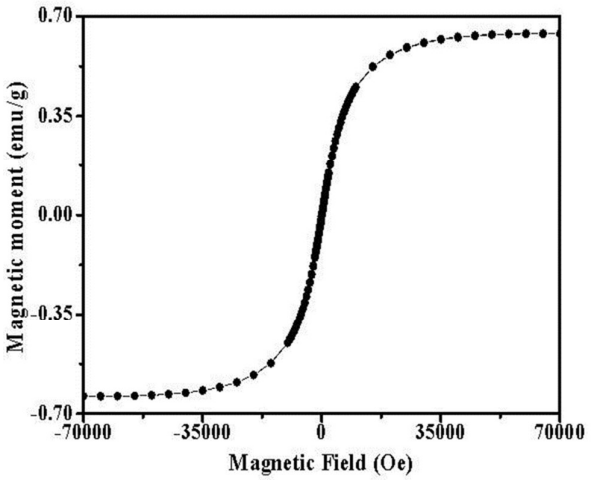

Fig. 7 SQUID magnetization of Fe_3O_4-loaded mPEG-b-P(DPA-DE)LG micelles at 300K.

approximately 0.06 emu g^{-1}, indicating that the Fe_3O_4-loaded mPEG-b-P(DPA-DE)LG micelles could potentially be used as MRI contrast agents. As shown in Supporting Information Figure S5A, the Fe_3O_4-loaded mPEG-b-P(DPA-DE)LG micelles were well-dispersed in the aqueous solution and showed a black-brown color at 0 hours with an applied magnetic field. However, the solution became clear, and the nanoparticles were accumulated near the magnet after 2 hours of the applied magnetic field (Figure. S5B). This result further illustrates the superparamagnetic performance of the Fe_3O_4-loaded mPEG-b-P(DPA-DE)LG micelles.

The relaxation property of the Fe_3O_4-loaded mPEG-b-P(DPA-DE)LG micelles in PBS was assessed to evaluate their potential as MRI contrast agents. As shown in Figure 8, when measuring the relaxation rate R (1/T) of the Fe_3O_4-loaded mPEG-b-P(DPA-DE)LG micelles as a function of iron concentration, the specific relaxivity was 0.704 mM^{-1} s^{-1} and 106.7 mM^{-1} s^{-1} for r_1 and r_2, respectively, which suggests ability as a T_2 contrast enhancing agent. The T_2-weighted MRI signals of the Fe_3O_4-loaded mPEG-b-P(DPA-DE)LG micelles are also shown in Figure 8. For the given iron concentrations ($\geqslant$0.05 mM), the contrast agent showed dark images,

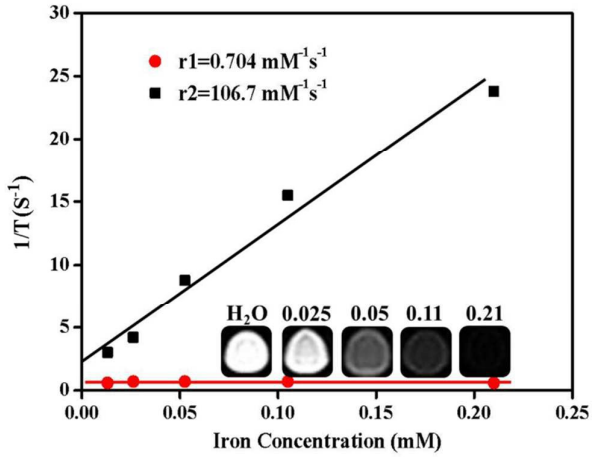

Fig. 8 Relaxation rate r (1/T, s^{-1}) as a function of iron concentration (mM) and corresponding T_2-weighted MRI images of Fe_3O_4-loaded mPEG-b-P(DPA-DE)LG micelles.

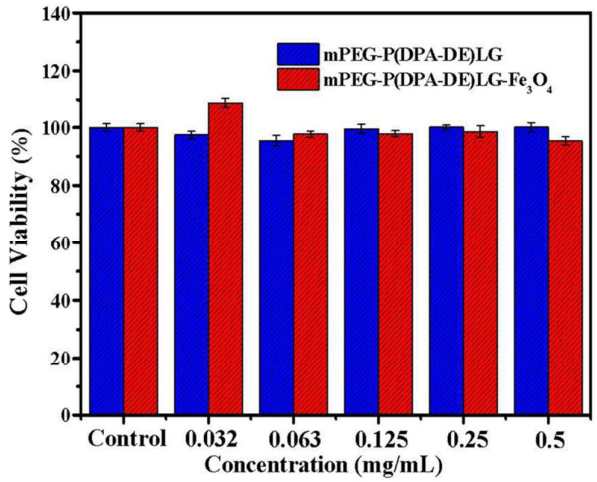

Fig. 9 The in vitro cytotoxicity evaluation of mPEG-b-P(DPA-DE)LG micelles and Fe_3O_4-loaded mPEG-b-P(DPA-DE)LG micelles on the HepG2 cells incubated by an MTT assay.

indicating that it can be used as a T_2-weighted contrast agent for MRI.

The in vitro cytotoxicity of the Fe_3O_4-loaded mPEG-b-P(DPA-DE)LG micelles and blank mPEG-b-P(DPA-DE)LG micelles was assessed using an MTT assay. HepG2 (human hepatocellular carcinoma) cell lines were utilized. Notably, the Fe_3O_4-loaded mPEG-b-P(DPA-DE)LG micelles and empty mPEG-b-P(DPA-DE)LG micelles did not show any cytotoxicity in the HepG2 cells, even at concentrations of up to 500 μg/mL (Figure 9). These results indicated that the Fe_3O_4-loaded mPEG-b-P(DPA-DE)LG micelles exhibited excellent safety and biocompatibility compared with empty mPEG-b-P(DPA-DE)LG micelles.

3.5 Release behaviour and cellular uptake of DOX–loaded mPEG-b-P(DPA-DE)LG micelles

A hydrophobic fluorescent agent DOX was encapsulated into the mPEG-b-P(DPA-DE)LG micelles using a solvent-evaporation

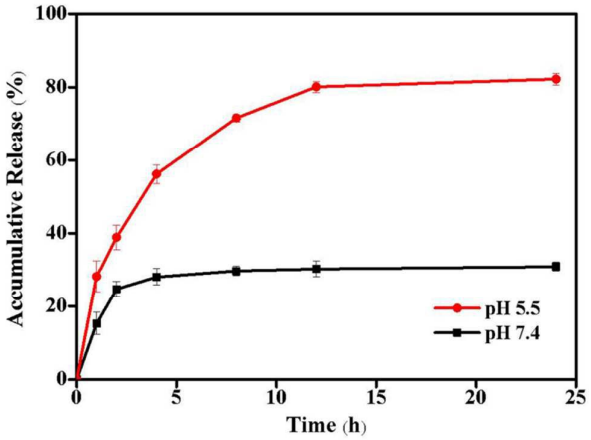

Fig. 10 The in vitro release profiles of DOX from DOX–loaded mPEG-b-P(DPA-DE)LG micelles at different pH values (7.4 and 5.5) at 37 °C measured by UV-vis spectroscopy.

method and the DLC and DLE of DOX into the mPEG-b-P(DPA-DE)LG micelles were 3.8% and 37.4%, respectively. The DOX release behaviour of the DOX-loaded mPEG-b-P(DPA-DE)LG micelles was investigated using a dialysis method at 37 °C in PBS at different pH values (7.4 and 5.5). As shown in Figure 10, the accumulative release of DOX in the physiological (pH 7.4) buffer reached approximately 30% within 4 h, and no tendency of further release was observed until 24 h. However, the DOX release rates were accelerated at acidic pH (pH 5.5), and over 80% of the loaded DOX was released within 24h due to the destabilization of micelles at a weakly acidic environment.

To further determine whether the pH responsive behaviour of the mPEG-b-P(DPA-DE)LG micelles would be advantageous for their internalization, DOX-loaded mPEG-b-P(DPA-DE)LG micelles were investigated in HepG2 cells by CLSM. As shown in Figure 11, after 1 h of incubation, the weak red fluorescence intensity of DOX-loaded mPEG-b-P(DPA-DE)LG micelles was observed in the cell nuclei in the merged image, which was the result of the slower rate of the energy-dependent endocytosis of the polymeric particles.[52] As the incubation time increased (from 1 h to 24 h), a much stronger red fluorescence intensity was exhibited by the DOX-loaded mPEG-b-P(DPA-DE)LG micelles in the cell nuclei in the merged image, indicating rapid internalization of the DOX-loaded mPEG-b-P(DPA-DE)LG micelles due to the demicellization of the polymeric micelles. These results suggested that the possibility of the pH-responsive mPEG-b-P(DPA-DE)LG copolymer could act as a smart carrier suitable for simultaneously targeting and releasing imaging agents in response to the acidic environment of pathologic tissues.

3.6 In vivo MR imaging

To test the ability of the Fe_3O_4-loaded mPEG-b-P(DPA-DE)LG micelles to act as pH-triggered targeting MRI agents, we employed a type of cerebral ischemia disease rat model with acidic tissue. The classic concept of ischemia is that the pH of the pathological tissue is lower than that of the normal tissue due to the accumulation of the lactic acid produced by anaerobic glycolysis[53, 54], which provides an acidic pH environment. Rats were subjected to middle cerebral artery occlusion (MCAO) in the right hemisphere resulting in an

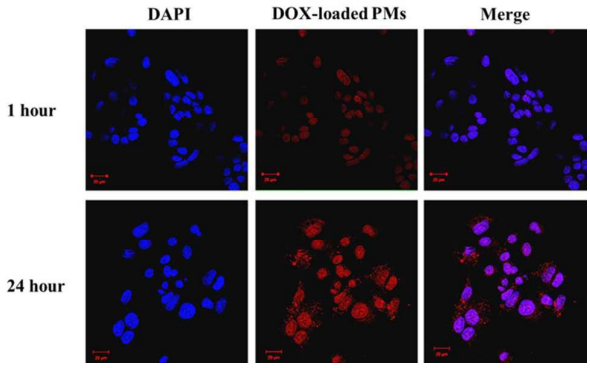

Fig. 11. confocal images of HepG2 cells incubated with DOX–loaded mPEG-b-P(DPA-DE)LG micelles (DOX-loaded PMs) at 1hour and 24 hour.

ischemic acidic region. The T_2-weighted MR imaging of the ischemic section of the brain of mice with MCAO at pre-treatment, 1, 3 and 24 h after intravenous injection of the Fe_3O_4-loaded mPEG-b-P(DPA-DE)LG micelles solution (20 mg Fe_3O_4 nanoparticles per kg of rat body weight) are shown in Figure 12 a. These results demonstrated the gradual accumulation of Fe_3O_4 nanoparticles in an area that is acidic due to ischemia (circle). As the blood brain barrier is destroyed as a consequence of ischemic vascular injury[55], Fe_3O_4-loaded mPEG-b-P(DPA-DE)LG micelles can be delivered to the acidic ischemic brain area, and after demicellization, naked Fe_3O_4 nanoparticles accumulate in the acidic pathologic area. In the control group, Fe_3O_4 nanoparticles were loaded into a non pH-responsive mPEG-b-P(DPA)LG micelles, and we found that the no signal decreased in the acidic pathologic area due the Fe_3O_4-loaded a non-pH responsive mPEG-b-P(DPA)LG micelles cannot happen demicellization, as shown in Figure 12 b. In the rats that only pH-responsive mPEG-b-P(DPA-DE)LG micelles, no signal decreases were observed in the ischemic and normal brain sites (Figure 12 c). This in vivo MRI data prove that the Fe_3O_4-loaded mPEG-b-P(DPA-DE)LG micelles can successfully and simultaneously target image acidic pathological tissue by a stimuli-responsive mechanism with pH as the stimulus.

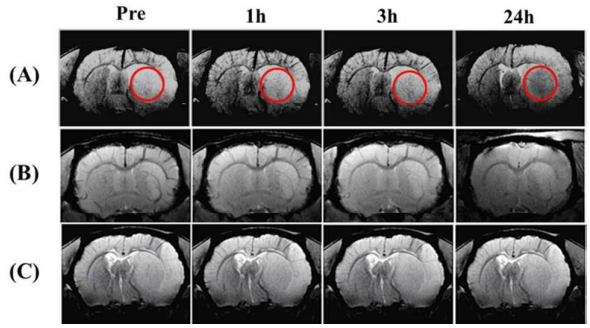

Fig. 12 T_2-weighted MR imaging of the rat brain with MCAO treatment, enhanced by (A) Fe_3O_4-loaded mPEG-b-P(DPA-DE)LG, (B) Fe_3O_4-loaded mPEG-b-P(DPA)LG as a control group, and (C) mPEG-b-P(DPA-DE)LG copolymer. The Fe_3O_4-loaded mPEG-b-P(DPA-DE)LG was dissolved in the acidic area of the ischemic brain and dark images gradual become deep over time (red circle) due to Fe_3O_4 nanoparticles were accumulated.

4 Conclusion

We demonstrated a new type of pH-responsive copolymer, which was used to carry Fe_3O_4 nanoparticles and act as a pH-triggered contrast agent for MR imaging. These novel Fe_3O_4-loaded mPEG-b-P(DPA-DE)LG micelles facilitate cell uptake and exhibit long-term stability and low cytotoxicity. The mPEG-b-P(DPA-DE)LG micelle can well encapsulate Fe_3O_4 nanoparticles at physiological pH (~7.4) with a high loading efficiency of 91.6% and a small particle size of ~120 nm. Consequently, the pH-responsive mPEG-b-P(DPA-DE)LG micelle can rapidly release Fe_3O_4 nanoparticles in response to an acidic pH-stimuli environment. Moreover, the Fe_3O_4-loaded mPEG-b-P(DPA-DE)LG micelles allow excellent T_2-weighted MR diagnostic imaging in an acidic ischemic brain area. These results suggest that, due to their unique acid-triggered abilities, the pH-responsive mPEG-b-P(DPA-DE)LG copolymers may have more applications in the biomedical field from MR diagnostic imaging to therapeutics for other acidic pathologic tissues.

Acknowledgments

This research was supported by the Basic Science Research Program through a National Research Foundation of Korea grant funded by the Korean Government (MEST) (20100027955). Prof. GuangHui Gao is grateful to the National Natural Science Foundation of China for a research support (NSFC) (No. 51473023).

Notes and references

1 Z. Qiao and X. Shi, *Prog. Polym. Sci*, 2015, **44**, 1.
2 G. H. Gao, J. W. Lee, M. K. Nguyen, G. H. Im, J. Yang, H. Heo, P. Jeon, T. G. Park, J. H. Lee and D. S. Lee, *J. Control. Release*, 2011, **155**, 11.
3 H. Cai, X. An, J. Cui, J. Li, S. Wen, K. Li, M. Shen, L. Zheng, G. Zhang and X. Shi, *ACS. Appl. Mater. Inter*, 2013, **5**, 1722.
4 K. Welsher and H. Yang, *Nat. Nanotechnol*, 2014, **9**, 198.
5 N. K. Logothetis, J. Pauls and A. Oeltermann, *Nature*, 2001, **412**, 150.
6 R. Popovtzer, A. Agrawal, N. A. Kotov and R. Kopelman, *Nano. Lett*, 2008, **8**, 4593.
7 P. Thibault, M. Dierolf, A. Menzel and F. Pfeiffer, *Science*, 2008, **321**, 379.
8 D. F. Cheng, Y. Wang, X. R. Liu, P. P. Pretorius, M. M. Liang and D. J. Hnatowich, *Bioconjugate. Chem*, 2010, **21** 1565.
9 L. Cheng, J. Liu, X. Gu, H. Gong, X. Shi, T. Liu, C. Wang, X. Wang, G. Liu, H. Xing, W. Bu, B. Sun and Z. Liu, *Adv. Mater*, 2014, **26**, 1886.
10 A. Gimelli, M. Bottai, D. Genovesi, A. Giorgetti, F. Di Martino and P. Marzullo, *Eur. J. Nucl. Med. Mol. I*, 2012, **39** 83.
11 E. S. Lee, A. S. Kamlet, D. C. Powers, C. N. Neumann, J. M. Hooker and T. Ritter, *Science*, 2011, **334**, 639.
12 M. H. Pablico-Lansigan, S. F. Situ and A. C. Samia, *Nanoscale*, 2013, **5**, 4040.
13 K. Lansing, D. G. Amen and C. Hanks, *J. Neuropsych. Clin. N.,* 2005, **17**, 526.
14 R. Bleul, R. Thiermann, G. U. Marten, M. J. House, T. G. St Pierre, U. O. Hafeli and M. Maskos, *Nanoscale*, 2013, **5**, 11385.
15 I. Tirotta, V. Dichiarante, C. Pigliacelli, G. Cavallo, G. Terraneo, F. B. Bombelli, P. Metrangolo and G. Resnati, *Chem. Rev.*, 2015, **115**, 1106.
16 R. M. Ferguson, K. R. Minard, K. M. Krishnan, *J. Magn. Magn. Mater.*, 2009, **321**, 1548.
17 J. Borgert, J. D. Schmidt, I. Schmale, J. Rahmer, C. Bontus, B. Gleich, B. David, R. Eckart, O. Woywode, J. Weizenecker, J. Schnorr, M. Taupitz, J. Haegele, F. M. Vogt and J. Barkhausen, *J. Cardiovasc. Comput.*, 2012, **6**, 149.
18 E. U. Saritas, P. W. Goodwill, L. R. Croft, J. J. Konkle, K. Lu, B. Zheng and S. M. Conolly, *J. Magn. Reson.*, 2013, **229**, 116.
19 A. K. Gupta and M. Gupta, *Biomaterials*, 2005, **26**, 3995.
20 M. Mahmoudi, S. Sant, B. Wang, S. Laurent and T. Sen, chemotherapy, *Adv. Drug. Deliver. Rev.*, 2011, **63**, 24.
21 C. He, X. Zhuang, Z. Tang, H. Tian and X. Chen, *Adv. Healthc. Mater.*, 2012, **1**, 48.
22 H. Lu, J. Wang, Z. Song, L. Yin, Y. Zhang, H. Tang, C. Tu, Y. Lin and J. Cheng, *Chem. Commun.*, 2014, **50**, 139.
23 J. Huang and A. Heise, *Chem, Soc, Rev*, 2013, **42**, 7373.
24 F. C. Smits, B. C. Buddingh, M. B. Eldijk and J. C. Hest, *Macromol. Biosci.*, 2015, **15**, 36.
25 J. R. Kramer and T. J. Deming, *J. Am. Chem. Soc.*, 2014, **136**, 5547.
26 A. P. Majewski, A. Schallon, V. Jerome, R. Freitag, A. H. Muller and H. Schmalz, *Biomacromolecules*, 2012, **13**, 857.
27 J. H. Maeng, D. H. Lee, K. H. Jung, Y. H. Bae, I. S. Park, S. Jeong, Y. S. Jeon, J. H. Kim, W. H. Kim and S. S. Hong, *Biomaterials*, 2010, **31**, 4995.
28 A. Pourjavadi, S. H. Hosseini, M. Alizadeh and C. Bennett, *Colloid. Surface. B.*, 2014, **116**, 49.
29 G. Marcelo, A. Muñoz-Bonilla, J. Rodríguez-Hernández and M. Fernández-García, *Polym. Chem.*, 2013, **4**, 558.
30 Z. Xu, Y. Feng, X. Liu, M. Guan, C. Zhao and H. Zhang, *Colloid. Surface. B.*, 2010, **81**, 503.
31 T. J. Deming, *Adv. Drug. Deliver. Rev.*, 2002, **54**, 1145.
32 T. J. Deming, *Prog. Polym. Sci.*, 2007, **32**, 858.
33 Y. Li, G.H. Gao and D.S. Lee, *J. Polym. Sci. Pol. Chem.*, 2013, **51**, 4175.
34 M. Guo, Y. Yan, H. Zhang, H. Yan, Y. Cao, K. Liu, S. Wan, J. Huang and W. Yue, *J. Mater. Chem.*, 2008, **18**, 5104.
35 Y. Li, G. H. Gao and D. S. Lee, *Adv. Healthc. Mater.*, 2013, **2**, 388.
36 B. Chang, X. Sha, J. Guo, Y. Jiao, C. Wang and W. Yang, *J. Mater. Chem.*, 2011, **21**, 9239.
37 E. S. Lee, Z. Gao, Y. H. Bae, *J. Control. Rel.*, 2008, **132**, 164–170.
38 R. Duncan, *Nat. Rev. Drug Discov.*, 2003, **2**, 347–360.
39 M. Stubbs, P. M. J. McSheehy, J. R. Griffiths, C. L. Bashford, *Mol. Med. Today.*, 2000, **6**, 15–19.
40 S. Yu, G. Wu, X. Gu, J. Wang, Y. Wang, H. Gao and J. Ma, *Colloid. Surface. B.*, 2013, **103**, 15.
41 L. Zhu, D. Wang, X. Wei, X. Zhu, J. Li, C. Tu, Y. Su, J. Wu, B. Zhu and D. Yan, *J. Control. Release.*, 2013, **169**, 228.
42 H. Wen, J. Guo, B. Chang and W. Yang, *Eur. J. Pharm. Biopharm.*, 2013, **84**, 91.
43 H. Lu and J. J. Cheng, *J. Am. Chem. Soc*, 2007, **129**, 14114.
44 L. Zhou, J. Yuan and Y. Wei, *J. Mater. Chem.*, 2011, **21**, 2823.
45 F. M. Veronese and G. Pasut, *Drug. Discov. Today.*, 2005, **10**, 1451.
46 H. S. Lee, S. M. Dellatore, W. M. Miller and P. B. Messersmith, *Science*, 2007, **318**, 426.
47 S. H. Sun, H. Zeng, D. B. Robinson, S. X. Wang, and G. X. Li, *J. Am. Chem. Soc.*, 2004, **126**, 273.
48 S. H. Sun and H. Zeng, *J. Am. Chem. Soc,* 2002, **124**, 8204.
49 B. R. Hao, R. J. Xing, Z. C. Xu, Y. L. Hou and S. H. Sun, , *Adv. Mater,* 2010, **22**, 2729.

50 J. X. Ding, X. L. Zhuang, C. S. Xiao and X. S. Chen, *J. Mater. Chem.*, 2011, **21**, 11383.
51 H. Ai, C. Flask, X. T. Shuai and J. M. Gao, *Adv. Mater.*, 17 2005, **17**, 1949.
52 G. J. M. Habraken, K. H. R. M. Wilsens, C. E. Koninga and A. Heise, *Polym. Chem.*, 2011, **2**, 1322.
53 S. J. Yu, J. X. Ding, C. L. He, Y. Cao, W. G. Xu and X. S. Chen, *Adv. Healthc. Mater.*, 2014, **3**, 752.
54 Z. G. Xiong, X. M. Zhu, X. P. Chu and R. P. Simon, *Cell*, 2004, **118**, 687.
55 J. Gao, B. Duan, D. G. Wang and T. L. Xu, *Neuron*, 2005, **48**, 635.